Solid–liquid interfacial energy of dichlorobenzene

2007 J. Phys.: Condens. Matter 19 116202

(http://iopscience.iop.org/0953-8984/19/11/116202)

J. Phys.: Condens. Matter **19** (2007) 116202 (11pp) doi:10.1088/0953-8984/19/11/116202

Solid–liquid interfacial energy of dichlorobenzene

U Böyük[1], **K Keşlioğlu**[2] **and N Maraşlı**[2,3]

[1] Department of Science Education, Education Faculty, Erciyes University, 38039 Kayseri, Turkey
[2] Department of Physics, Faculty of Arts and Sciences, Erciyes University, 38039 Kayseri, Turkey

E-mail: marasli@erciyes.edu.tr

Received 21 December 2006
Published 27 February 2007
Online at stacks.iop.org/JPhysCM/19/116202

Abstract

Commercial-purity dichlorobenzene was purified using a columnar distillation system. The equilibrated grain boundary groove shapes for purified dichlorobenzene (DCB) were directly observed by using a temperature gradient stage. From the observed grain boundary groove shapes, the Gibbs–Thomson coefficient and solid–liquid interfacial energy of purified DCB were determined to be $(6.2 \pm 0.6) \times 10^{-8}$ K m and $(29.3 \pm 4.4) \times 10^{-3}$ J m^{-2} with the present numerical model and the Gibbs–Thomson equation, respectively. The grain boundary energy of the DCB phase was determined to be $(54.1 \pm 9.2) \times 10^{-3}$ J m^{-2} from the observed grain boundary grooves. The thermal conductivity ratio of the liquid phase to the solid phase was measured to be 0.94.

1. Introduction

The solid–liquid interfacial energy, σ_{SL}, is the reversible work required to form or to extend a unit area of interface between a crystal and its coexisting liquid and plays a central role in determining the nucleation rate and growth morphology of crystals [1–3]. Thus, a quantitative knowledge of σ_{SL} values is necessary. The measurement of σ_{SL} in pure materials and alloys is difficult. Over the last half-century, various attempts have been made to determine the mean value of the solid–liquid interfacial free energy in variety of materials [1–31]. More recently, a technique for the quantification of interfacial free energy from the solid–liquid interfacial grain boundary groove shape has been established, and measurements have been reported for several systems [7–31]. These measurements of groove shape in a thermal gradient can be used to determine the interfacial energy independently of the grain boundary energy, because the interface near the groove must everywhere satisfy

$$\Delta T_r = \left[\frac{1}{\Delta S^*}\right]\left[\left(\sigma_{SL} + \frac{d^2\sigma_{SL}}{dn_1^2}\right)\kappa_1 + \left(\sigma_{SL} + \frac{d^2\sigma_{SL}}{dn_2^2}\right)\kappa_2\right], \quad (1)$$

[3] Author to whom any correspondence should be addressed.

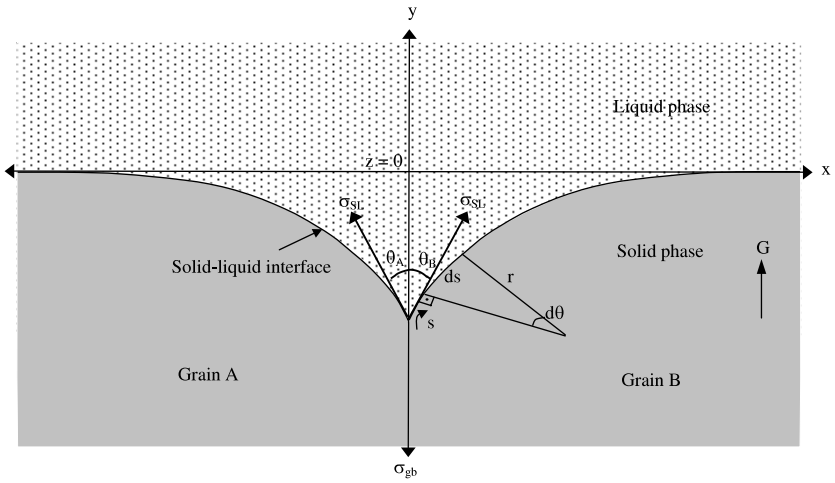

Figure 1. Schematic illustration of an equilibrated grain boundary groove formed at a solid–liquid interface in a temperature gradient showing the x, y coordinates and angle θ.

where ΔT_r is the curvature undercooling, ΔS^* is the entropy of fusion per unit volume, $n = (n_x, n_y, n_z)$ is the interface normal, κ_1 and κ_2 are the principal curvatures, and the derivatives are taken along the directions of principal curvature. Thus, the curvature undercooling is a function of curvature, interfacial free energy and the second derivative of the interfacial free energy. Equation (1) is valid only if the interfacial free energy per unit area is equal to the surface tension per unit length, $\sigma_\mathrm{SL} = \gamma$. When surface energy differs from surface tension the problem is more complicated and the precise modification of the Gibbs–Thomson equation has not yet been established [4]. When the solid–liquid interfacial free energy is isotropic, equation (1) becomes

$$\Delta T_\mathrm{r} = \frac{\sigma_\mathrm{SL}}{\Delta S^*}\left(\frac{1}{r_1} + \frac{1}{r_2}\right), \tag{2}$$

where r_1 and r_2 are the principal radii of curvature. For the case of a planar grain boundary intersecting a planar solid–liquid interface, $r_2 = \infty$ and equation (2) becomes

$$\Gamma = r\,\Delta T_\mathrm{r} = \frac{\sigma_\mathrm{SL}}{\Delta S^*}, \tag{3}$$

where Γ is the Gibbs–Thomson coefficient. This equation is called the Gibbs–Thomson relation.

Equation (3) may be integrated in the y direction (perpendicular to the macroscopic interface) from the flat interface to a point on the cusp

$$\int_0^y \Delta T_\mathrm{r}\,\mathrm{d}y = \Gamma \int_0^y \frac{1}{r}\,\mathrm{d}y. \tag{4}$$

The right-hand side of equation (4) may be evaluated for any shape by defining $\mathrm{d}s = r\,\mathrm{d}\theta$ (s is the distance along the interface and θ is the angle of the interface to y as shown in figure 1) giving

$$\int_0^y \frac{1}{r}\,\mathrm{d}y = (1 - \sin\theta). \tag{5}$$

The left-hand side of equation (4) may be evaluated if ΔT_r is known as a function of y.

The left-hand side of equation (4) was integrated numerically using the values of ΔT_r calculated numerically and the right-hand side was evaluated by measuring the value of θ (obtained by fitting a Taylor expansion to the adjacent points on the cusp) by Gündüz and Hunt [15, 16]. This allows the Gibbs–Thomson coefficient to be determined for a measured grain boundary groove shape. This numerical method calculates the temperature along the interface of a measured grain boundary groove shape rather than attempting to predict the equilibrium grain boundary groove shape. The shape of the interface, the temperature gradient in the solid, G_S and the ratio of thermal conductivity of the liquid phase to solid phase, $R = K_L/K_S$, must be known or measured to get accurate values of the Gibbs–Thomson coefficient with the Gündüz and Hunt numerical method.

One of the common techniques for measuring the solid–liquid interfacial free energy is the method of grain boundary grooving in a temperature gradient. In this technique, the solid–liquid interface is equilibrated with a grain boundary in a temperature gradient as shown in figure 1, and the mean value of the solid–liquid interfacial free energy is obtained from measurements of the equilibrium shape of the groove profile. The grain boundary groove method is the most useful and powerful technique currently available for measuring the solid–liquid interfacial free energy and can be applied to measure σ_{SL} for multi-component systems as well as pure materials, for opaque materials as well as transparent materials, for any observed grain boundary groove shape and for any $R = K_L/K_S$ value. Over last 25 years, the equilibrated grain boundary groove shapes in a variety of materials have been observed and measurements of solid–liquid interfacial free energies have been made from observed grain boundary groove shapes [7–30].

Although dichlorobenzene (DCB) has a similar solidification structure to metallic materials it has not been used as an organic analogue material because some of its thermophysical properties, such as its solid–liquid interfacial energy, Gibbs–Thomson coefficient and thermal conductivity, have not been determined or are not known. No attempts have been made to determine the solid–liquid interfacial free energy and Gibbs–Thomson coefficient for DCB. Thus the goal of the present work was to determine the thermal conductivity ratio of the liquid phase to solid phase, the Gibbs–Thomson coefficient, the solid–liquid interfacial energy and the grain boundary energy for purified DCB.

2. Experimental procedures

2.1. Preparation of test materials

The experimental technique requires the preparation of thin slides containing the high-purity test material and the necessary thermocouple assemblies. Accordingly, the preparation of specimens for purified transparent material involved three primary operations: (i) the purification of test materials by distillation, (ii) the design and assembly of the thin-slide specimen cell and (iii) filling the specimen cell with the purified test material under a vacuum. The relevant details regarding these procedures are given below.

Commercial purity DCB was purified in quantities of approximately 100 cm^3 using a columnar distillation system as shown in figure 2. The condensation temperature for purified DCB was 383 K. The distillation was repeated four times, and the distilled material was finally collected in a glass tube, flame-sealed under a vacuum during the distillation. The melting-temperature of purified DCB was measured to be 326.6 K with a standard route under a vacuum.

The specimen cells were fabricated such that the test material was contained between two parallel ground glass plates, each being 0.12 mm thick, 50 mm long and 24 mm wide. A silicone elastomer glue was used to attach and seal the assembly on three sides with four K-

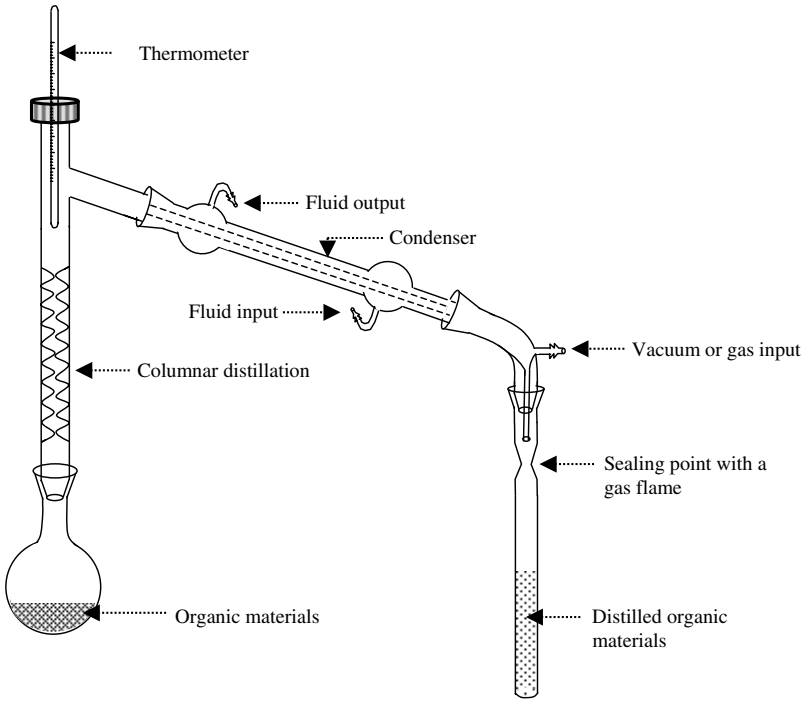

Figure 2. The columnar distillation system used to purify the test materials.

type thermocouples (50 μm in diameter) fixed within the cell and distributed along the length direction with a spacing of 2–3 mm. The distance between the two glass plates was 60–80 μm. Before filling the cell with DCB, the glue was cured for at least 24 h at room temperature to avoid any reaction between the test material and the glue.

Test specimens were prepared by the remelting of purified DCB material under a vacuum followed by the introduction of the material into the prepared glass cells. During this procedure, the material was kept within a specialized filling chamber designed to minimize contamination from ambient air, as shown in figure 3. Before remelting, the chamber atmosphere was evacuated and the test material then melted. Within the filling chamber, the open end of the test cell was immersed into the liquid DCB, and argon gas with a pressure of approximately 15 bar applied to force-fill the thin slide. After filling, the slide was permitted to cool until it was completely solid. The specimen was removed from the chamber and the unsealed edge sealed.

2.2. The temperature gradient measurement

Bayender *et al* [19] utilized a temperature gradient stage to observe the equilibrated grain boundary groove shape in transparent organic materials. In the present work, a similar apparatus was employed to observe the solid DCB in equilibrium with its melts. The apparatus consisted of hot and cold stages as shown in figure 4.

The hot stage comprises two copper plates which are resistively heated by NiCr wires, insulated in alumina tubes and integrally threaded through the plates of the hot stage. A total of 1000 mm of heater wire, 0.5 mm in diameter was used in the hot stage, providing a maximum power of 4500 W at 220 V AC. To maximize the thermal stability of the hot stage,

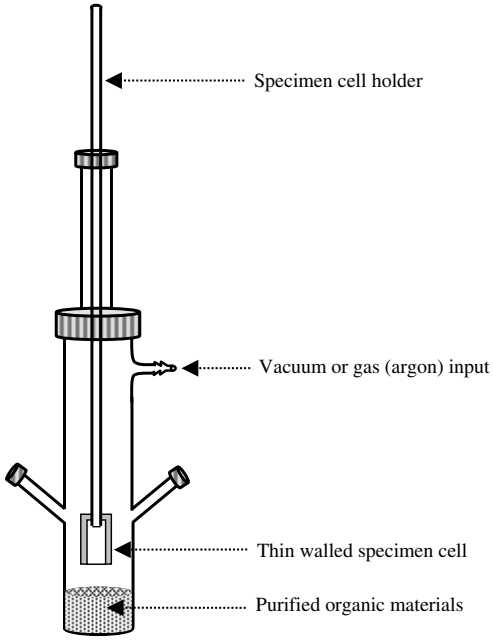

Figure 3. Schematic illustration of the filling chamber.

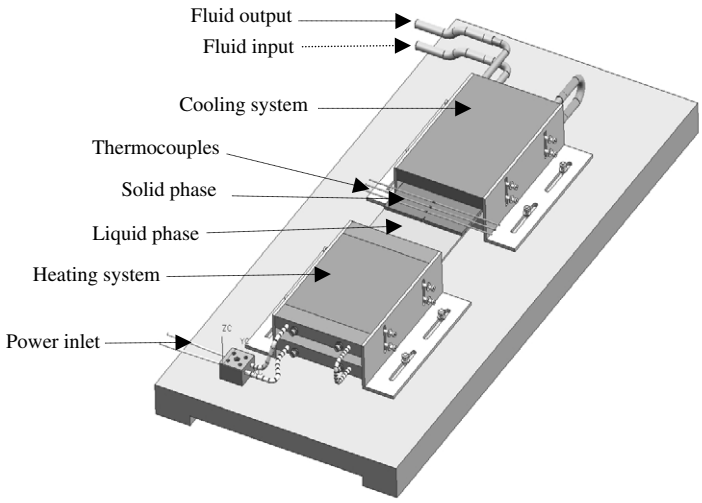

Figure 4. Schematic illustration of the horizontal temperature gradient stage.

a transformer was placed in the supply circuit, stepping the maximum current down to 4 A. A fully proportional thermistor-based control system was implemented, employing a control thermocouple within the hot stage. The temperature of the hot stage was controlled to an accuracy of ± 0.01 K with a *Eurotherm 2604* type controller.

The design of the cold stage is similar to that of the hot stage. However, cooling is achieved using a *PolyScience digital 9102* model heating/refrigerating circulating bath containing an aqueous ethylene glycol solution. The temperature of the circulating baths was kept constant at 283 K to an accuracy ± 0.01 K.

A thin liquid layer (2 or 3 mm thick) was melted and the specimen was held in a constant temperature gradient to observe the solid DCB in equilibrium with its melt. The equilibrating time for the purified DCB was 1 day. When the solid–liquid interface reached equilibrium, the temperature difference between two thermocouples, ΔT, was measured using a Hewlett-Packard model 34401A digital multimeter. The multimeter has a 1 μV resolution for direct voltage measurements. The positions of the thermocouples and the equilibrated grain boundary groove shapes were then photographed with a *Honeywell CCD* digital camera placed in conjunction with an *Olympus BH2* type light optical microscope. The distance between the two thermocouples, ΔX, was measured from the photographs of the thermocouple positions using Adobe PhotoShop version 8.0 software.

The temperature gradient, $G = \Delta T/\Delta X$, for the equilibrated grain boundary groove shapes was determined using the values of ΔT and ΔX. The estimated error in the measurements of temperature gradient, G, is about 5% [21].

The coordinates of the equilibrated grain boundary groove shapes were measured with an optical microscope to an accuracy of ± 10 μm. The uncertainty in the measurements of equilibrated grain boundary groove coordinates was 0.1%.

2.3. Thermal conductivity ratio of liquid phase to solid phase

The thermal conductivity ratio of the liquid phase to the solid phase for purified DCB, $R = K_L/K_S$, must be known or measured to evaluate the Gibbs–Thomson coefficients with the present numerical method. The thermal conductivity ratio can be obtained during directional growth with a Bridgman type growth apparatus. The heat flow away from the interface through the solid phase must balance that liquid phase plus the latent heat generated at the interface, i.e. [32]

$$VL = K_S G_S - K_L G_L, \tag{6}$$

where V is the growth rate, L is the latent heat, G_S and G_L are the temperature gradients in the solid and liquid, respectively, and K_S and K_L are the thermal conductivities of solid and liquid phases, respectively. For very low velocities, $VL \ll K_S G_S$, so that the thermal conductivity ratio, R, is given by

$$R = \frac{K_L}{K_S} = \frac{G_S}{G_L}. \tag{7}$$

A directional growth apparatus, first constructed by McCartney [33], was used to find out the thermal conductivity ratio, $R = K_L/K_S$. A thin walled glass tube, 5 mm OD, 3 mm ID and 180 mm total length, was used to minimize the convection in the liquid phase. Molten purified DCB was poured into the thin walled glass tube and the molten DCB was then directionally frozen from bottom to top to ensure that the crucible was completely full. The specimen was then placed in the directional growth apparatus.

The specimen was heated to 15 K over the melting temperature of purified DCB. The specimen was then left to reach thermal equilibrium for at least 2 h. The temperature in the specimen was measured with an insulated K-type thermocouple. In the present work, a 1.2 mm OD, 0.8 mm ID alumina tube was used to insulate the thermocouple from the melts and the thermocouple was placed perpendicular to the heat flow (growth) direction. At the end of equilibration, the temperature in the specimen was stable to ± 0.5 K for a short term period and to ± 1 K for a long term period. When the specimen temperature stabilized, the directional growth was begun by turning the motor on. The cooling rate was recorded with a data logger via a computer. In the present measurements, the growth rate was 8.3×10^{-4} cm s^{-1}. When the solid–liquid interface passed the thermocouple, a change in the slope of the cooling rate for

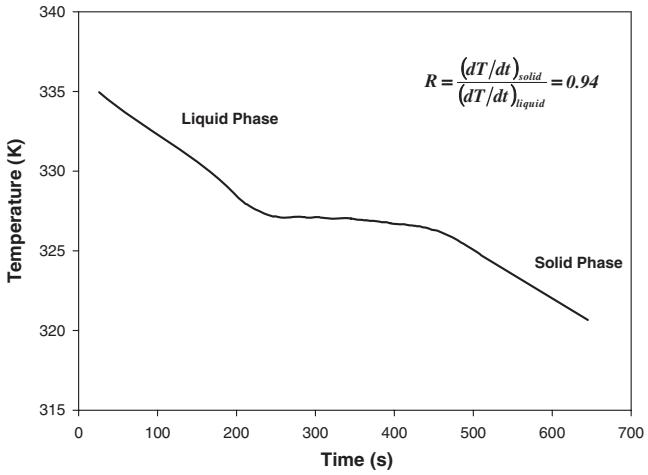

Figure 5. Cooling rate of purified DCB.

the liquid and solid phases was observed. When the thermocouple reading was approximately 5 K below the melting temperature, the growth was stopped by turning the motor off.

The thermal conductivity ratio can be evaluated from the cooling rate ratio of the liquid phase to the solid phase. The cooling rate of the liquid and solid phases is given by

$$\left(\frac{\mathrm{d}T}{\mathrm{d}t}\right)_{\mathrm{L}} = \left(\frac{\mathrm{d}T}{\mathrm{d}x}\right)_{\mathrm{L}} \left(\frac{\mathrm{d}x}{\mathrm{d}t}\right)_{\mathrm{L}} = G_{\mathrm{L}} V, \tag{8}$$

and

$$\left(\frac{\mathrm{d}T}{\mathrm{d}t}\right)_{\mathrm{S}} = \left(\frac{\mathrm{d}T}{\mathrm{d}x}\right)_{\mathrm{S}} \left(\frac{\mathrm{d}x}{\mathrm{d}t}\right)_{\mathrm{S}} = G_{\mathrm{S}} V. \tag{9}$$

From equations (7)–(9), the thermal conductivity ratio can be written as

$$R = \frac{K_{\mathrm{L}}}{K_{\mathrm{S}}} = \frac{G_{\mathrm{S}}}{G_{\mathrm{L}}} = \frac{\left(\frac{\mathrm{d}T}{\mathrm{d}t}\right)_{\mathrm{S}}}{\left(\frac{\mathrm{d}T}{\mathrm{d}t}\right)_{\mathrm{L}}}, \tag{10}$$

where $(\mathrm{d}T/\mathrm{d}t)_{\mathrm{S}}$ and $(\mathrm{d}T/\mathrm{d}t)_{\mathrm{L}}$ values were directly measured from the temperature versus time curve shown in figure 5. The thermal conductivity ratio of the liquid phase to the solid phase for purified DCB was found to be 0.94 from figure 5. The estimated error in the measurements of the thermal conductivity of the solid and liquid phases was about 5% [34].

3. Results and discussion

3.1. The Gibbs–Thomson coefficient

If the thermal conductivity ratio of the equilibrated liquid phase to solid phase, $R = K_{\mathrm{L}}/K_{\mathrm{S}}$, the coordinates of the grain boundary groove shapes and the temperature gradient in the solid phase G_{S} are known, then the Gibbs–Thomson coefficient can be obtained using the numerical method described in detail in [15]. The experimental error in the determination of the Gibbs–Thomson coefficient is the sum of experimental errors of the measurements of the temperature gradient and thermal conductivity. Thus the total error in the determination of the Gibbs–Thomson coefficient was about 10%.

Table 1. Gibbs–Thomson coefficients for purified DCB in equilibrium with its melts. The subscripts LHS and RHS refer to the left-hand side and right-hand side of the groove, respectively.

		Gibbs–Thomson coefficient Γ (K m)	
Groove No	$G_S \times 10^2$ (K m^{-1})	$\Gamma_{LHS} \times 10^{-8}$	$\Gamma_{RHS} \times 10^{-8}$
a	51.6	6.1	6.1
b	46.6	6.2	6.1
c	58.0	6.3	6.2
d	53.7	6.0	6.2
e	19.7	6.3	6.3
f	17.7	6.1	6.2
g	14.7	6.2	6.3
h	17.9	6.1	6.1
i	18.1	6.2	6.1
j	22.3	6.2	6.1

Table 2. Some thermophysical properties of DCB.

Materials	DCB
Melting point, T_M	326.6 K
Molecular weight, m	147×10^{-3} kg mol^{-1}
Density	1.241×10^3 kg m^{-3}
Molecular volume, V_S	118.45×10^{-6} m^3 mol^{-1}
Enthalpy change, ΔH_M	18.3×10^3 J mol^{-1} [39]
Entropy of fusion, ΔS^*	4.74×10^5 J K^{-1} m^{-3}

The Gibbs–Thomson coefficients for solid DCB in equilibrium with its melts were determined by the numerical method using 10 observed grain boundary groove shapes and the results are given in table 1. Typical grain boundary groove shapes for purified solid DCB in equilibrium with its melts examined in the present work are shown in figure 6.

The mean value of Γ with experimental error from table 1 is $(6.2 \pm 0.6) \times 10^{-8}$ K m for purified solid DCB.

3.2. The entropy of fusion per unit volume

To determine the solid–liquid interfacial free energy it is also necessary to know the entropy of fusion per unit volume; this is given by

$$\Delta S^* = \frac{\Delta H_M}{T_M} \frac{1}{V_S}, \tag{11}$$

where ΔH_M is the enthalpy change of the solid phase at the melting temperature, T_M is the melting temperature and V_S is the molar volume of the solid phase. The values of T_M, V_S and ΔS^* are given in table 2. The error in the determination of entropy of fusion per unit volume is estimated to be about 5% [35].

3.3. The solid–liquid interfacial energy

If the values of the Gibbs–Thomson coefficient and the entropy of fusion per unit volume are measured or known, the solid–liquid interfacial energy can be obtained from equation (3). The experimental error in the determination of the solid–liquid interfacial energy is the sum

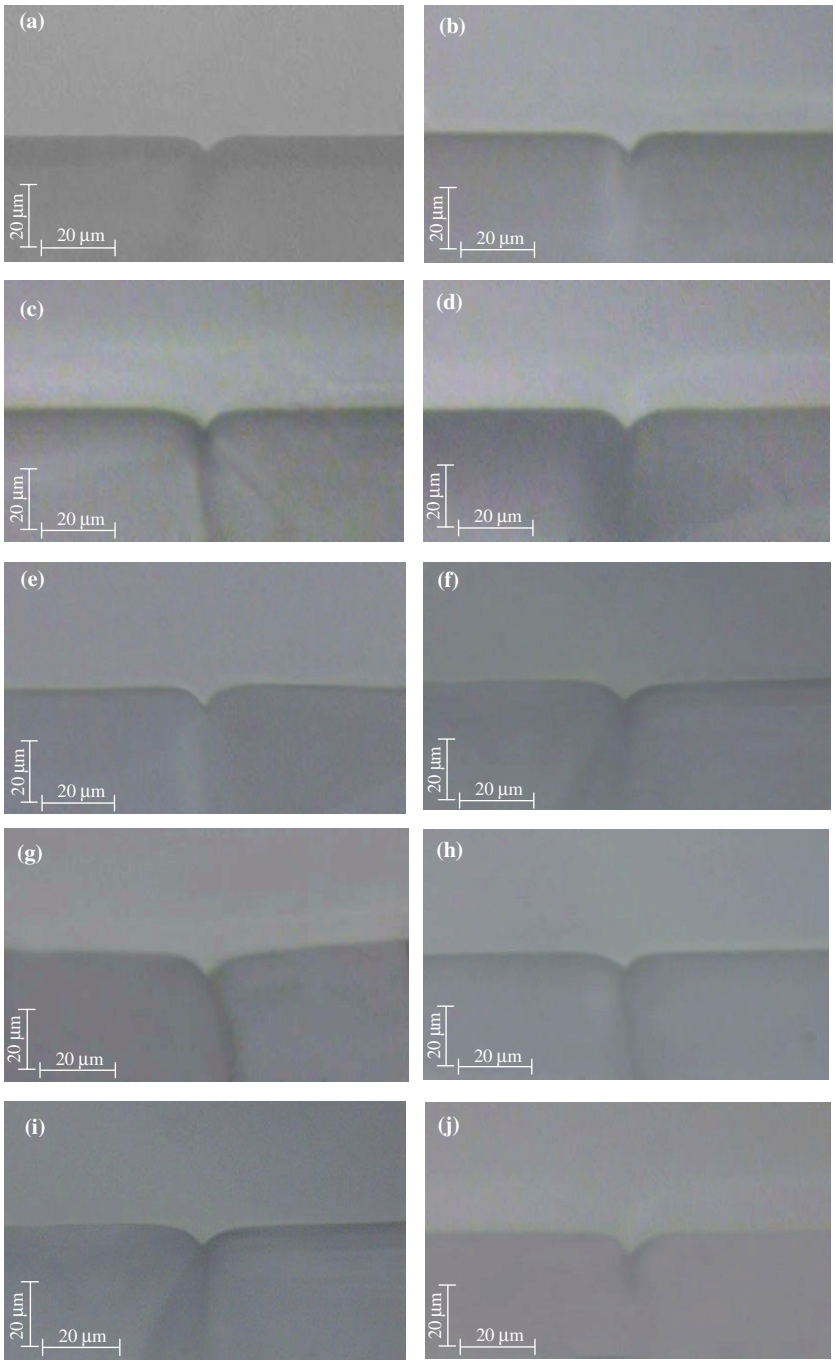

Figure 6. Typical grain boundary groove shapes for purified DCB.

of the experimental errors of the Gibbs–Thomson coefficient and the entropy of fusion per unit volume. Thus the total experimental error in the determination of the solid–liquid interfacial energy with the present method was about 15%. The mean value of the solid–liquid

Table 3. A comparison of the calculated values of σ_{SL} with the experimental values of σ_{SL} for some organic materials.

			Solid–liquid interface energy, $\sigma_{SL} \times 10^{-3}$ (J m^{-2})	
Organic materials	ΔH (J mol^{-1})	$V_S \times 10^{-6}$ (m^3 mol^{-1})	Calculated with equation (12)	Experimental
Succinonitrile	3 484 [37]	76.50	7.9	7.9 [21]
(D) Camphor	6 865 [37]	153.80	9.6	10.8 [24]
Pivalic acid	2 427 [14]	112.70	4.2	2.7 [19]
				2.8 [14]
Camphene	2 706 [36]	161.80	3.7	4.4 [20]
Pyrene	16 600 [38]	159.13	22.8	21.9 [31]
Dichlorobenzene	18 300 [39]	118.45	30.6	29.3 ± 4.4 (present work)

interfacial energy, σ_{SL}, for purified solid DCB in equilibrium with its melts was found to be $(29.3 \pm 4.4) \times 10^{-3}$ J m^{-2}.

Based on nucleation experiments and classical nucleation theory, Turnbull [1] proposed an empirical relationship between the interfacial energy and melting enthalpy change to estimate the interfacial energy, expressed as [1]

$$\sigma_{SL} = \frac{\tau \Delta H_M}{V_S^{2/3} N_a^{1/3}}, \tag{12}$$

where the coefficient τ was found to be 0.45 for metals and 0.34 for nonmetallic systems [1] and N_a is the Avogadro constant. Comparisons of the calculated values of σ_{SL} by equation (12) with the experimental values of σ_{SL} for different organic materials are given in table 3. As can be seen from table 3, the calculated values of σ_{SL} are in good agreement with the experimental values of σ_{SL} except for pivalic acid.

3.4. The grain boundary energy

The grain boundary energy can be expressed by

$$\sigma_{gb} = 2\sigma_{SL} \cos\theta, \tag{13}$$

where $\theta = \frac{\theta_A + \theta_B}{2}$ is the angle that the solid–liquid interfaces make with the y-axis [40]. The angles θ_A and θ_B were obtained from the cusp coordinates x, y using a Taylor expansion for parts at the base of the groove. The mean value of grain boundary energy was then calculated from equation (13) using the mean value of the solid–liquid interfacial energy and the values of θ. The estimated error in the determination of the angles was found to be 2% from standard deviation. Thus the total experimental error in the resulting grain boundary energy is about 17%. The mean value of σ_{gb} for purified solid DCB was found to be $(54.1 \pm 9.2) \times 10^{-3}$ J m^{-2}.

4. Conclusions

The grain boundary groove shapes for purified DCB were directly observed with a horizontal temperature gradient stage. From the observed grain boundary groove shapes, the Gibbs–Thomson coefficient, the solid–liquid interfacial energy and the grain boundary energy for purified DCB were determined to be $(6.2 \pm 0.6) \times 10^{-8}$ K m, $(29.3 \pm 4.4) \times 10^{-3}$ J m^{-2} and $(54.1 \pm 9.2) \times 10^{-3}$ J m^{-2}, respectively. The thermal conductivity ratio of the liquid phase to the solid phase for purified DCB was also measured to be 0.94.

Acknowledgments

This project was supported by Erciyes University Scientific Research Project Unit under contract number FBA-04-3. The authors are grateful to Erciyes University Scientific Research Project Unit for their financial support.

References

[1] Turnbull D 1950 *J. Appl. Phys.* **21** 1022
[2] Jones D R H 1974 *J. Mater. Sci.* **9** 1
[3] Jackson C L and McKenna G B 1990 *J. Chem. Phys.* **93** 9002
[4] Trivedi R and Hunt J D 1993 *The Mechanics of Solder Alloy Wetting and Spreading* (New York: Van Nostrand-Reinhold) p 191
[5] Morris J R and Napolitano R E 2004 *JOM* **56** 40
[6] Hoyt J J, Asta M, Haxhimali T, Karma A, Napolitano R E and Trivedi R 2004 *MRS Bull.* **29** 935
[7] Jones D R H and Chadwick G A 1970 *Phil. Mag.* **22** 291
[8] Jones D R H and Chadwick G A 1971 *J. Cryst. Growth* **11** 260
[9] Jones D R H 1978 *Phil. Mag.* **27** 569
[10] Schaefer R J, Glicksman M E and Ayers J D 1975 *Phil. Mag.* **32** 725
[11] Hardy S C 1977 *Phil. Mag.* **35** 471
[12] Nash G E and Glicksman M E 1971 *Phil. Mag.* **24** 577
[13] Bolling G F and Tiller W A 1960 *J. Appl. Phys.* **31** 1345
[14] Singh N B and Glicksman M E 1989 *J. Cryst. Growth* **98** 573
[15] Gündüz M and Hunt J D 1985 *Acta Metall.* **33** 1651
[16] Gündüz M and Hunt J D 1989 *Acta Metall.* **37** 1839
[17] Maraşlı N and Hunt J D 1996 *Acta Mater.* **44** 1085
[18] Stalder I and Bilgram J H 2003 *J. Chem. Phys.* **118** 798
[19] Bayender B, Maraşlı N, Çadırlı E, Sişman H and Gündüz M 1998 *J. Cryst. Growth* **194** 119
[20] Bayender B, Maraşlı N, Çadırlı E and Gündüz M 1999 *Mater. Sci. Eng.* A **270** 343
[21] Maraşlı N, Keşlioğlu K and Arslan B 2003 *J. Cryst. Growth* **247** 613
[22] Böyük U, Keşlioğlu K, Erol M and Maraşlı N 2005 *Mater. Lett.* **59** 2953
[23] Keşlioğlu K, Böyük U, Erol M and Maraşlı N 2006 *J. Mater. Sci.* **41** 7939
[24] Ocak Y, Akbulut S, Böyük U, Erol M, Keşlioğlu K and Maraşlı N 2006 *Scr. Mater.* **55** 235
[25] Ocak Y, Akbulut S, Böyük U, Erol M, Keşlioğlu K and Maraşlı N 2006 *Thermochim. Acta* **55** 235
[26] Keşlioğlu K and Maraşlı N 2004 *Mater. Sci. Eng.* A **369** 294
[27] Keşlioğlu K and Maraşlı N 2004 *Metall. Mater. Trans.* A **35A** 3665
[28] Erol M, Maraşlı N, Keşlioğlu K and Gündüz M 2004 *Scr. Mater.* **51** 131
[29] Keşlioğlu K, Erol M, Maraşlı N and Gündüz M 2004 *J. Alloys Compounds* **385** 207
[30] Erol M, Keşlioğlu K and Maraşlı N 2007 *Metall. Mater. Trans.* A at press
[31] Akbulut S, Ocak Y, Böyük U, Erol M, Keşlioğlu K and Maraşlı N 2007 *J. Appl. Phys.* **100** 123505
[32] Porter D A and Easterling K E 1991 *Phase Transformations in Metals and Alloys* (UK: Van Nostrand-Reinhold) p 204
[33] McCartney D G 1981 *D Phil Thesis* University of Oxford UK, p 85
[34] Erol M, Keşlioğlu K, Şahingöz R and Maraşlı N 2005 *Met. Mater. Int.* **11** 421
[35] Tassa M and Hunt J D 1976 *J. Cryst. Growth* **34** 38
[36] Rubinstein E R and Glicksman M E 1991 *J. Cryst. Growth* **112** 97
[37] Witusiewicz V T, Sturz L, Hecht U and Rex S 2004 *Acta Mater.* **52** 4561
[38] Rai U S and Pandley P 2003 *J. Cryst. Growth* **249** 301
[39] Rai R N and Rai U S 2000 *Thermochim. Acta* **363** 23
[40] Woodruff P 1973 *The Solid–Liquid Interface* (Cambridge: Cambridge University Press)